Empirical oscillating potentials for alloys from ab-initio fits and the prediction of quasicrystal-related structures in the Al–Cu–Sc system

Marek Mihalkovič[1,2] and C. L. Henley[1]

[1] *Laboratory of Atomic and Solid State Physics, Cornell University, Ithaca, NY, 14853-2501*
[2] *Permanent address, Institute of Physics, Slovak Academy of Sciences, 84228 Bratislava, Slovakia.*

By fitting to a database of ab-initio forces and energies, we can extract pair potentials for alloys, with a simple six-parameter analytic form including Friedel oscillations, which give a remarkably faithful account of many complex intermetallic compounds. Furthermore, such potentials are combined with a method of discovering complex zero-temperature structures with hundreds of atoms per cell, given only the composition and the constraint of known lattice parameters, using molecular–dynamics quenches. We apply this approach to structure prediction in the Al–Cu–Sc quasicrystal-related system.

PACS numbers: 02.70.Ns,61.50.Lt,63.20.Dj,64.70.Kb,61.44.Br

Various problems in materials modeling can only be addressed by "empirical" interatomic potentials[1]. Say we wish to evaluate a physical property (e.g. total energy) of some material with a complex crystal structure. We cannot directly insert the results of crystallographic refinements, as they (almost always) include sites with mixed or fractional occupancies. To obtain valid results, we must assign those occupancies plausibly based on computed energy differences. A single relaxation with fast ab-initio codes such as VASP[2] may be tractable in a cell of 10^3 atoms; however, if (say) 5% of those atoms are uncertain, this must be repeated many times to find the one optimum state out of 2^{50} possibilities.

But with empirical, approximate potentials that can be evaluated in negligible time, this optimization is tractable, and can be followed up by ab-initio relaxation to obtain the most accurate positions and total energies. When combined with effective search algorithms, such as genetic algorithms or the "cell–constrained melt–quench" method (presented in Sec. II) this is a powerful tool for ab-initio structure discovery. Some other questions that call for empirical potentials are phonon spectra (or other dynamics), and thermodynamic simulations of phase transformations in complex alloys.

A popular framework of empirical potentials is the "embedded-atom method" (EAM)[3,4], in which the full Hamiltonian contains the usual pair term $V_{ij}(r_i - r_j)$, but also an implicitly many-atom term $\sum_i U(\rho(r_i))$, where $\rho(r_i)$ is a sum of contributions at atom i from nearby atoms. Accurate EAM potentials are straightforward to extract for pure elements,but demand patience and skill to obtain even for binary systems; there is no *systematic* recipe for multicomponent systems.

Here we present an alternative approach fitting only pair interactions but incorporating Friedel oscillations. These "empirical oscillating pair potentials" (EOPP) have the form[6]

$$V(r) = \frac{C_1}{r^{\eta_1}} + \frac{C_2}{r^{\eta_2}} \cos(k_* r + \phi_*) \qquad (1)$$

All six parameters, including k_*, are taken as independent in the fit for each pair of elements. Eq. (1) was inspired by effective potentials (e.g. Refs. 7 and 8) used in previous work on structurally complex metals, e.g. quasicrystals[9,10]. In such systems, energy differences between competing structures are often controlled by second- and third-neighbor wells due to Friedel oscillations, which are a consequence (mathematically) of Fourier transforming the Fermi surface, or (physically) are equivalent to the Hume-Rothery stabilization by enhancing the strength of structure factors that hybridize states across the Fermi surface.[11] In Pettifor's framework (Ref. 11, Sec. 6.6), the short-range repulsion is captured by the first term of (1); the medium-range potential (first-neighbor well) as well as the long-range oscillatory tail are captured by the second term, their relative weights being adjusted by the η_1 and η_2 parameters. Since the second term has this double duty of representing both the nearest-neighbor and long-distance behaviors, the fitted $1/r^{\eta_2}$ decay generally does not agree with analytic asymptotic result of $1/r^3$; also, k_* need not match the Fermi wavevector, and these parameters take different values for the six kinds of pair potentials.

In the rest of this Letter, we describe how our potentials are fitted (typically for a particular composition range) and then demonstrate their capabilities through case studies in the alloy system Al–Cu–Sc, which has local order similar to the binary quasicrystal i(CaCd) or to Zn-rich Mg–Zn alloys. Along with this, we also describe a method of "constrained cell quenching" that accesses low-energy structures in surprisingly large cells. Finally, we will summarize other systems where EOPP have been applied, and discuss their limitations.

I. DATABASE AND POTENTIAL FITTING

The parameters in Eq. (1) are fitted to an ab-initio dataset (using the VASP code[2]) combining both relaxed $T = 0$ structures and molecular dynamics (MD) simulations at high T. Four criteria in choosing structures for the database are (1) to bracket the composition range of interest; (2) to mix simple and complex structures; (3) to ensure adequately many contacts of every kind (in particular, nearest neighbors of the least abundant species); (4) to have similar atom densities[12]. In ab-initio MD simulations of the simpler structures, a supercell is always used with dimensions comparable to the fitting potential cutoff radius, which (for the fit procedure) is always 12Å .

We define each structure's energy as a difference relative to a coexisting mixture (with the same total composition) of

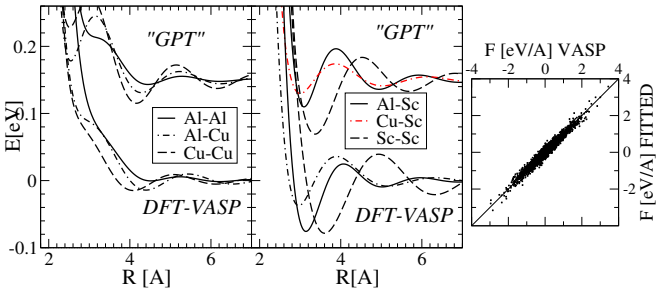

FIG. 1: (a). *Top*: EOPP form (Eq. 1) fitted to "GPT" potentials (Ref. 16); the fitted/GPT curves lie exactly on the top of each other. The Cu–Sc potential is not available from Ref. 8; the figure shows a fit to ab–initio data with the other five pairs constrained to GPT form. *Bottom*: the EOPP form fitted to VASP force and energy data. The curves fitted to "GPT" are shifted by 0.15 eV/atom for clarity. (b). Scatter plot of the forces for the EOPP fit to [Eq. (1)], from the fitted Al-Cu-Sc potentials shown in (a), bottom. The pair potential forces $\mathbf{F}_j$ are vertical axis, ab-initio data horizontal.

reference phases, chosen to bracket all database compositions. Every structure is used for both forces (from MD at high T) and energy differences[13] (high-T MD, as well as relaxed at $T = 0$). For the high-T portion, we took one snapshot of each structure at the end of a short ab-initio MD run. Usually $\gtrsim 10^3$ force components enter the fit, along with ~ 50 energy differences. Typical forces are ~ 3 eV/Å and typical energy differences are ~ 0.3 eV/atom; the fit residuals are $\sim 5\%$ and $\sim 1\%$ respectively [see e.g. Fig. 1(a)].

Our least-squares fit minimizes (by the Levenberg-Marquardt algorithm) $\chi^2 \equiv \sum \Delta E_i^2/{\sigma_E}^2 + \sum |\Delta \mathbf{F}_j|^2/{\sigma_F}^2$, where $\{\Delta E_i\}$ and $\{\Delta \mathbf{F}_j\}$ are the energy and force residuals; we found a weighting ratio $\sigma_E/\sigma_F \sim 10^{-3}$Å was optimal so that neither energies nor forces dominate the fit.

There is some risk of converging to a false minimum (or not converging at all, from an unreasonable initial guess). Thus, it is important to repeat the fit from several starting guesses. For this we used, e.g., potentials first fitted to pure elements or binary systems, and also used a library of parameter sets previously fitted for some different alloy system. The fitted parameters in (1) for each of our examples are available as supplementary information[6]; similar potentials were plotted in Refs. 14 (for Al-Mg) and 15 (for Sc-Zn).

For our specific case of Al–Cu–Sc, our database had 84 relaxed energies at $T = 0$K from (besides the pure elements) the binaries Al_3Sc.cP4, Cu_2Sc.tI6, Al_2Sc.cF24, and Al_2Cu.cF12 and ternaries AlCuSc.hP12, $Mg_2Cu_6Ga_5$.cP39 (with Mg→Sc, Ga→Al), and $AlCrCu_2$.cF16 (with Cr→Sc); structures are identified by Pearson labels. The database also had 7428 force points at $T > 0$K, taken from all those structures, and additionally from Al_2Sc.hP12, and $Sc(Al_{1-x}Cu_x)_6$.cI168. The EOPP potentials give very good agreement with this database, as shown in Figure 1(a): the r.m.s. deviation of forces was 0.11 eV/Å and that of energy differences was 21.7 meV/atom, with relative weights set to maximize accuracy of the force data.[5] Values of the parameters are listed in Table I, Appendix A.

Our empirical potentials can be compared with Moriarty's "GPT" potentials [16], derived from a systematic expansion, which are known for all but one of the six Al–Cu–Sc pair potentials [see Fig. 1(b)]. First, when the GPT potentials are fitted to the EOPP form (Eq. (1), the curves virtually lie on top of each other: thus, the EOPP form *can* represent all features of the GPT potentials. Second, the GPT and EOPP potentials show a strong similarity; the main mismatches are (i) EOPP has no first-neighbor well for Al–Cu and Cu–Cu (ii) the oscillation wavelength for Sc-Sc differs (iii) the overall energy scale of the GPT pair potential is too small by ∼50%.[17]. In practice empirically fitted potentials account for some of the many-body contributions by modifying their pair terms, and hence work better than truncating a systematic expansion (e.g. GPT[16]) after the pair terms.

II. CONSTRAINED-CELL MELT QUENCHING

We now turn to the second method which, together with fitted potentials, has enabled the present structure study and others. In many alloy systems, with no structural information known except the composition *and the unit cell*, structures with > 100 atoms per cell may be predicted from careful "melt quenching" (MQ) simulations. The relation to the EOPP notion is that the larger systems – particularly when supercells are used – are too large for direct ab-initio calculations, so empirical potentials are crucial for melt-quenching. This method has been applied with GPT potentials to improve known structures of the decagonal Al–Co–Ni quasicrystals[18].

In most cases, annealing requires "tempering Monte Carlo (MC)"[19] wherein ~ 10 samples are annealed simultaneously at equally spaced temperatures spanning across the melting temperature. Each tempering cycle includes a short MD run (~ 1 ps with 1 fs steps) followed by lattice-gas MC annealing (~ 200 attempts per atom) in which the chemical identities of two randomly selected atoms may be swapped. Then, pairs of samples may be swapped using a Metropolis-like criterion. (For the Al–Cu–Sc structures we studied, our temperatures spanned 600–1700 K with spacing ΔT =100K, and the interaction cutoff was set to $r_{cut} = 9$Å.) The resulting structure may be tested subsequently by ab-initio calculations of the total energy, for which we used VASP[2].

A key diagnostic in a tempering simulation is the (time-dependent) energies $E_m(t)$ of all samples, as specific heat is approximately $\Delta E/\Delta T$, where $\Delta E = E_{m+1} - E_m$. For our structures ΔE peaked around T =1400K, indicating the melting point. In our cases with 52 or 84 atoms per primitive cell, *several* independently initialized runs yielded identical low-T structures, which took 100–200 cycles.

III. TARGET STRUCTURES

We now apply empirical pair potentials and cell-constrained melt-quenching to realistic structure prediction in the Al–Cu–Sc system, for two newly discovered phases[20,21]

in which lattice parameters were known from electron microscopy but no single-grain structures were available for structure determination. We label each phase by its Pearson symbol. These belong to a family of phases in which atom size is the salient attribute: Ca, Mg, Sc, and rare earths are "large" atoms, constituting $\sim 1/6$ by number; whereas Al, Zn, Cu, and Cd are the majority "small" atoms.

Our first target is "$cI168$" with 84 atoms per primitive cell, hypothesized to be isostructural with the $ScZn_6$ phase. No single-crystal data are available; a preliminary Rietveld refinement of powder data technique[21] confirmed the $ScZn_6$ type structure, with refined lattice parameter a=13.52Å. The chemical ordering and occupancies of Al/Cu could not be determined reliably prior to our modeling[21].

The $ScZn_6$ phase is an "approximant" of the recently discovered thermodynamically stable, icosahedral quasicrystal i(ScZn), meaning its unit cell contents are identical to a fragment of the quasicrystal structure. i(ScZn) has the same atomic structure as i(CaCd)[22], which (along with similar rare earth-Cd quasicrystals) are the only known stable binary quasicrystals. Each site is specific to either a small atom (Cd or Zn) or a large atom (Sc, Ca, or rare earth).

Both $cI168$-$ScZn_6$ and the related quasicrystals are understood to be packings of a three-shell, icosahedrally symmetric cluster called the "Tsai cluster". Its outermost shell has an icosahedron of 12 large atoms plus 30 small atoms (forming an icosidodecahedron) on the midpoints of the large-large bonds [See Fig. 2(a)], and inside that is a dodecahedron of 20 small atoms. At the cluster center is a *tetrahedron* of small atoms; as this breaks the icosahedral symmetry, it has many degenerate orientations, which leads to interesting slow dynamics of reorientations[23] and to structural ordering transitions at low T in the related crystals.

Our second target is "$oC104$", of composition $Al_{38.8}Cu_{45.7}Sc_{15.5}$, Initially [20] the lattice parameters a=8.32Å, b=8.36Å, c=21.99Å and C-centered orthorhombic Bravais lattice were identified from powder data but that was insufficient to refine the structure.

IV. RESULTS: PHASE STABILITY AND PSEUDO-TSAI CLUSTERS

Constrained-cell melt-quenching using the same database-fitted EOPP potentials converged to low–temperature structures in both cases, the energies of which were subsequently evaluated by VASP. In the $cI168$ case this was the known structure. In the $oC104$ case, a previously unknown structure was obtained[6], computed unstable by only 5 meV/atom with respect to $cI168$; its validity was confirmed by a subsequent refinement of the powder data[20] with this as the starting point. This predicted structure had space group $Amm2$, in which there were 11 Cu, 7 Al and 4 Sc Wyckoff sites, with no chemical disorder.

The fundamental motif in both $cI168$ and $oC104$ is an icosahedral cluster whose innermost shell has less symmetry. In $cI168$ this is a Tsai cluster [Fig. 2 (a)] in which each of the three Al/Cu shells has composition $Al_{0.5}Cu_{0.5}$. Strikingly, within each shell, the Al and Cu are segregated into hemispheres centered on fivefold axis of the icosahedron[25]; furthermore, the Al parts of each shell overlay the Cu parts of the preceding one and vice versa [see Figure 2(a)] . Due to this symmetry breaking, one expects the low–temperature phase to have at least several equivalent domains, corresponding to different orientations of the pseudo-Tsai clusters.

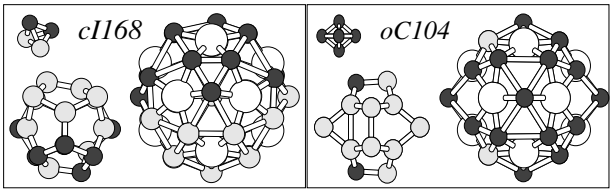

FIG. 2: (a) Tsai cluster in $cI168$ structure (left) and (b) "pseudo-Tsai" cluster (right) found in the $oC104$ structure. View along 2–fold direction. In each panel, the successive shells are (1) tetrahedron Al_2Cu_2 or octahedron Cu_6 (2) dodecahedron $(Al,Cu)_{20}$, and (3) icosidodecahedron $(Al,Cu)_{30}$ plus icosahedron Sc_{12}. Large white circles represent Sc, dark smaller circles Cu, and light smaller circles Al.

In the $oC104$ case we find a variant motif[26] that we call the "pseudo-Tsai" cluster, in which the innermost shell is a Cu_6 octahedron [Fig.2(b)]. This cluster was first described in Mg_2Zn_{11}.$cP39$[26], where the outer shell is a Zn_8Mg_{12} dodecahedron plus a Zn_{12} icosahedron[29].

The experimental (powder data) refinement[20] of $oC104$ is an *average* structure, with higher symmetry (space group $Cmmm$) than our model, accomodating 3 Sc Wyckoff sites, and 13 mixed Al/Cu sites (one of the latter being half-occupied). Each experimental site derives from one or two sites in our model, displaced on average by ∼0.17Å (Al), ∼0.12Å(Cu) and 0.08Å(Sc). Crystallographic data of the low–temperature model structure, are compared with the experimental structure in Appendix B. The mean deviation of the refined Al/Cu content from the averaged model content is 16%.

The electronic density of states for $cI168$ has a deep, narrow pseudogap at the Fermi energy, which tends to stabilize a unique composition. In contrast, $oC104$ has a shallower and wider pseudogap, suggesting a range of degenerate compositions, so that substitutional entropy might stabilize this phase at higher temperatures.

The pseudo-Tsai clusters in $oC104$ (and also the less complex $cP39$) adjoin by sharing atoms such that their centers are closer by a factor ~ 1.618 (golden ratio) than Tsai clusters would be. Could pseudo-Tsai clusters be the basis of the newly reported i(AlCuSc) quasicrystal[30]?

V. CONCLUSION.

We have shown that empirical potentials with the simple oscillating form (1), fitted from ab-initio data and combined

with a "cell constrained" brute-force quenching, allows detailed predictions of fairly complex low-temperature optimal structures in Al–Cu–Sc alloys, based on the very limited input of known lattice parameters and composition. Finding the correct structure depends sensitively on having a quantitatively realistic potential, which is achievable only if that potential is constructed or fitted from ab-initio calculations. One would expect that the oscillating analytical form (1) is natural only for simple metals (e.g. Al or Mg, for which it does very well). But in fact, the EOP potentials sometimes work quite well even when angular or many-body interactions are important, e.g. the transition metal neighbors in Al–Cu–Sc. But – not surprisingly – they do poorly for elemental Zn or Ga. Of course, *any* pair potential fails when the electron density has large variations in space (as at vacancies, edge dislocations, or surfaces), or in the (many) cases where bond directionality (due to covalent bonding) is prominent.

We believe the EOPP potentials are quite broadly applicable to mimic the atomic interactions of many metallic systems with sufficient accuracy to stand in for ab-initio energies when those would be computationally prohibitive. Although the EOP potentials were not formally presented before this paper, they have already been applied to a variety of intermetallics: (1) the site contents in complex structures, e.g. Al–Mg[14] or Al–Zn–Mg[32]; (2) solving the complete structures of complex Mg-rich Mg–Pd phases (with > 400 atoms/cell) in conjunction with diffraction, when the latter alone is insufficient[34]; (3) phonon spectra, e.g. in Zn–Sc[15] and Mg–Zn[26] alloys, and even in liquid Bi-Li alloys[31]; (4) the dynamics of the Tsai cluster tetrahedra in the $cI168$ structure $ScZn_6$[23], as well as the arrangements of the asymmetric inner Al_{10} shell in the pseudo-Mackay icosahedral clusters in quasicrystal-related Al–Ir, Al–Pd–Mn, and Al–Cu–Fe phases[33].

Acknowledgments

We thank R. G. Hennig and T. Ishimasa for discussions, and M. Widom for collaboration at an earlier stage. This work was supported by DOE Grant DE-FG02-89ER-45405 (MM, CLH), and Slovak funding VEGA 2/0111/11 and APVV-0647-10 (MM).

Appendix A: EOPP parameters for Al–Cu–Sc system.

The EOPP potential parameters fitting Eq.1 to DFT/VASP data are shown in Table I.

Appendix B: Crystallographic data of the $oC104$ structure

Table II lists Wyckoff orbits of the low–temperature structure, resulting from the melt–quenching procedure described in Sec. II, using EOPP Al–Cu–Sc potentials (Tab. I). The structure was subsequently optimized using DFT code VASP. The experimental (relaxed) cell parameters were a=8.3370 (8.3247) Å, b=22.0150 (21.868) Å and c=8.3370 (8.3247) Å, space group $Amm2$ (no. 38). Note that a and c axis are swapped with respect to the setting in Ref. 20. Column μ is site multiplicity, column ΔR shows displacement of the final relaxed atomic positions from the refined diffraction–data sites, and the last column (x_{Al}) is occupancy by Al atom from Ref. 20. The experimentally determined structure has higher symmetry (space group $Cmmm$), and shows averaging over disorder manifested at M2 site, forming 0.8Å–distant pairs of half–occupied positions. Occupancy of the M2 site couples with Al/Cu symmetry breaking of its adjacent M8a/b and M9a/b sites – all other sites marked a/b in the table (Sc3, M3, M10 and M13) have unique chemical assignement. Not surprisingly, largest displacement ΔR from the $Cmmm$ diffraction–data model occurs for Al–occupied variants of the M8 and M9 sites (Cu is stronger X–ray scatterer). The average $Cmmm$ model can be therefore interpreted as thermal average over (locally) ordered patterns, in which flip of the M2 atom by $\sim$0.8 Å over pseudo–mirror plane perpendicular to c axis at z=0 is correlated with Al$\equiv$Cu swap of adjacent M8a/M8b and M9a/M9b sites.

[1] "Empirical potentials" are explicit, classical functions of coordinates, not requiring an eigenvalue calculation.

[2] (a) G. Kresse and J. Hafner, Phys. Rev. B, 47, R558 (1993); (b) G. Kresse and J. Furthmuller, Phys. Rev. B 54, 11169 (1996).

[3] M. S. Daw and M. I Baskes, Phys. Rev. B 29, 6443 (1984).

[4] M. I. Baskes, Phys. Rev. Lett. 59, 2666 (1987); see e.g. B. Jelinek *et al*, Phys. Rev. B 75, 054106 (2007).

[5] An alternative weighting favoring accuracy in the energies would decrease the r.m.s. deviation for the energy datapoints to 7.9 meV/atom, while increasing the r.m.s. deviation of the force data to 0.15 eV/Å.

[6] Tables of parameters in Eq. (1) for Al–Cu–Sc, as well as the crystal structure of the $oC104$ phase, will be placed in supplementary material on arxiv.org.

[7] J. Hafner, *From Hamiltonians to Phase Transitions* (Springer, Heidelberg, 1987).

[8] J. A. Moriarty and M. Widom, Phys. Rev. B 56, 7905 (1997).

[9] (a). M. Mihalkovič *et al* Phys. Rev. B 53, 9021 (1996); (b) M. Mihalkovič *et al*, Phys. Rev. B 65, 104205 (2002).

[10] M. Krajči and J. Hafner, Phys. Rev. B 46, 10669 (1992).

[11] D. Pettifor, *Bonding and Structure of Molecules and Solids* (Oxford Univ. Press, Cambridge, 1995).

[12] For a successful fit, the database must be limited to a relatively narrow range of (electron) densities, so the Fermi wavevector [hence k_* in Eq. (1)] has a consistent value. Even our high-T MD samples were constrained to have the *same* density as at $T = 0$, rather than the physical zero-pressure values.

[13] Fits from forces alone were insufficiently constrained; including energy differences, even with low weight, improved the fit.

[14] M. Feuerbacher *et al*, Z. Kristallogr. 222, 259 (2007)

[15] M. de Boissieu *et al*, Nature Mater. 6, 977 (2007).
[16] (a) J. A. Moriarty, Phys. Rev. B 16, 2537 (1977); (b). Phys. Rev. B 26, 1754 (1982).
[17] We observed a similar agreement between the GPT and EOPP fitted potentials in the Al-Co-Ni and Al-Cu-Fe systems.
[18] M. Mihalkovič, C. L. Henley, and M. Widom, Philos. Mag. 91, 2557 (2011).
[19] R. H. Swendsen and J. S. Wang, Phys. Rev. Lett. 57, 2607 (1986)
[20] T. Ishimasa, A. Hirao, T. Honma and M. Mihalkovič, Philos. Mag. 91, 2594 (2011).
[21] T. Ishimasa and T. Honma, personal communication.
[22] H. Takakura, C. P. Gomez, A. Yamamoto, M. de Boissieu, A. P. Tsai, Nat. Mat. 6, 58 (2007)
[23] M. Mihalkovič and C. L. Henley, Philos. Mag. 91, 2548 (2011)
[24] Q. Lin and J. D. Corbett, Inorg. Chem. 42, 8762 (2003).
[25] Properly "pseudo-fivefold", as this is in a cubic crystal.
[26] H. Euchner, M. Mihalkovič, *et al*, Phys. Rev. B 83, 144202 (2011).
[27] G. Bergman, J. L. T. Waugh, and L. Pauling, Acta Crystallogr. 10, 254 (1957).
[28] V. Elser and C. L. Henley, Phys. Rev. Lett. 55, 2883 (1985).
[29] In fact we find ternary variant of Mg_2Zn_{11}.cP39, the $Mg_2Cu_6Al_5$.cP39 structure stable, coexisting with the $cP168$ structure, at T=0K.
[30] T. Honma and T. Ishimasa, Philos. Mag. 87, 2721 (2007).
[31] J. F. Wax, M. R. Johnson, L. E. Bove, *et al.* Phys. Rev. B 83, 144203 (2011).
[32] M. de Boissieu and M. Mihalkovič, unpublished.
[33] M. Mihalkovič and C. L. Henley, unpublished; M. Mihalkovič, C. L. Henley, and M. Krajči, unpublished.
[34] G. Kreiner and M. Mihalkovič unpublished.

	C_1	η_1	C_2	η_2	k_*	Φ_*
Al–Al	372.35	7.310	-1.508	3.600	3.552	2.995
Al–Sc	459191.27	15.730	-17.912	4.656	3.363	1.693
Al–Cu	249.79	7.563	-1.563	3.025	2.937	5.812
Sc–Sc	18493.28	11.264	2.379	2.559	2.308	0.947
Sc–Cu	194.11	7.361	-10.462	4.255	2.721	4.548
Cu–Cu	1036.62	9.503	-0.875	2.818	3.095	6.052

TABLE I: Fitted parameters for Al–Cu–Sc EOPP potentials.

site	chem.	μ	X	Y	Z	ΔR	x_{Al}
Sc1	Sc	8	0.6942	0.8140	0	0.10	–
Sc2	Sc	4	0	0.3844	0.0008	0.03	–
Sc3a	Sc	2	0.5	0	0.3051	0.04	–
Sc3b	Sc	2	0.5	0	0.3086	0.07	–
M1	Cu	4	0.2564	0	-0.0064	0.07	0.05
M2[†]	Cu	4	0	0.2574	0.0414	0.03	0.96
M3a	Cu	2	0	0	0.2452	0.09	0.11
M3b	Cu	2	0	0.5	0.2322	0.09	0.11
M4	Cu	8	0.3465	0.4066	-0.0046	0.04	0.12
M5	Al	4	0.5	0.0687	-0.0014	0.04	0.88
M6	Cu	4	0	0.0661	-0.0152	0.17	0.22
M7	Cu	4	0.5	0.2490	0.2537	0.04	0.68
M8a	Cu	8	0.2408	0.3081	0.1583	0.05	0.28
M8b	Al	8	0.2144	0.2963	-0.1652	0.30	0.28
M9a	Cu	4	0	0.3446	-0.3383	0.01	0.15
M9b	Al	4	0	0.3240	0.3334	0.46	0.15
M10a	Cu	4	0.5	0.3689	0.2544	0.03	0
M10b	Cu	4	0.5	0.3684	-0.2560	0.01	0
M11	Al	4	0.1821	0.5	-0.0072	0.06	0.78
M12	Al	4	0.5	0.3050	0.0034	0.03	0.69
M13a	Al	8	0.2201	0.4187	0.2728	0.08	0.93
M13b	Al	8	0.2194	0.4199	-0.2820	0.07	0.93

[†] this site has 0.5 occupancy in the refinement Ref. 20.

TABLE II: List of Wyckoff sites for $oC104$ structure minimizing EOPP energy, starting from random initial state, and using fixed experimentally determined lattice parameters as the only input. Last two columns compare the refined structure with the Rietveld–refined structure of Ref. 20, see text.